Available online at www.sciencedirect.com
SCIENCE DIRECT
ELSEVIER
Scripta Materialia 55 (2006) 649–652
Scripta MATERIALIA
www.actamat-journals.com

Increased strain rate sensitivity due to stress-coupled grain growth in nanocrystalline Al

D.S. Gianola, D.H. Warner, J.F. Molinari and K.J. Hemker*

Department of Mechanical Engineering, Johns Hopkins University, Baltimore, MD 21218-2681, United States

Received 24 April 2006; revised 26 May 2006; accepted 1 June 2006

A combined experimental/simulation approach has been used to characterize the underlying deformation mechanisms associated with stress-assisted grain growth in nanocrystalline Al. Strain rate sensitivity experiments on freestanding submicron thin films undergoing stress-assisted grain boundary migration have uncovered rate sensitivities up to two orders of magnitude larger than previously reported for microcrystalline Al. Molecular dynamics simulations have been used to illustrate that these high strain rate sensitivities coincide with those associated with grain boundary processes such as migration, sliding, and dislocation nucleation.

Keywords: Nanocrystalline materials; Strain rate sensitivity; Grain boundary migration; Molecular dynamics; Thin films

The thermal stability of pure nanocrystalline (nc) materials has been questioned [1–3] in light of the large volume fraction of grain boundaries (GBs) that are present in the microstructure and the instability associated with such a meta-stable configuration. Nonetheless, synthesis techniques have been developed that result in nc-microstructures that are remarkably stable. The role of impurities in stabilizing microstructures is highlighted [4] by the fact that chemically synthesized nc-Al shows spontaneous grain growth if produced in a reducing atmosphere [5] but exhibits thermal stability when produced in the presence of impurities [6]. Evidence is emerging that underscores the influence of the applied stress on microstructural evolution in nc-metals, which points to a departure from previous descriptions of deformation mechanisms that are based on a stable microstructure. Although not universally reported in nc studies, rapid grain coarsening has been observed at room temperature [7,8] and in the absence of thermal activation (cryogenic temperatures) [9], and theoretical formulations have recently been developed that directly correlate applied shear stresses with normal GB migration [10,11].

This ability of shear stresses to directly couple to low and high angle GBs [10,12,13] and the ensuing grain growth has been shown to have a dramatic effect on the mechanical behavior of nc-Al [6], although the details surrounding the underlying mechanistic processes have yet to be elucidated. Here, we present experiments that probe the strain rate dependence of the mechanical behavior of nc-Al thin films that are undergoing stress-assisted discontinuous grain growth in an effort to shed light on the operating mechanisms. Experimentally measured strain rate sensitivities coupled with molecular dynamics (MD) simulations of planar Al GBs combine to illustrate that flow behavior involving GB migration is highly rate sensitive.

Submicron freestanding thin films were synthesized [6] using pulsed direct current magnetron sputtering of a 99.999% pure Al target at a base chamber pressure of 1×10^{-7} Torr. A tensile testing structure was designed and constructed using Si-based microfabrication techniques [6] that provide a platform for handling and mounting fragile freestanding thin films. A tensile modality for mechanical testing was chosen in order to achieve a uniaxial loading condition, which avoids complexities arising from strain gradients and concentrations associated with nanoindentation experiments [14,15]. A custom built microsample tensile testing apparatus [16], which offers precise grip alignment with five degrees of freedom, was utilized for mechanical testing.

Transient strain rate experiments provide a fingerprint of the deformation in crystalline materials by means of examining the thermal activation of plastic flow, usually expressed as quantities such as activation volume and strain rate sensitivity. Activation volume

* Corresponding author. Tel.: +1 410 516 4489; fax: +1 410 516 7254; e-mail: hemker@jhu.edu

1359-6462/$ - see front matter
doi:10.1016/j.scriptamat.2006.06.002

is usually expressed as the derivative of the activation enthalpy with respect to stress [17], i.e.

$$v^* = -\left(\frac{\partial \Delta H(\tau)}{\partial \tau}\right)_T = k_B T \left(\frac{\partial \ln \dot{\gamma}}{\partial \tau}\right)_T, \quad (1)$$

where ΔH is the activation enthalpy. A commonly used quantity is the strain rate sensitivity parameter m, defined as

$$m = \frac{\partial \ln \tau}{\partial \ln \dot{\gamma}}. \quad (2)$$

Strain rate jump experiments, which involve incrementally increasing the applied strain rate ($\dot{\gamma}$) and measuring the change in flow stress (τ) required to continue deformation, and monotonic strain rate tests were also employed to define these quantities. Al films with nominal thicknesses of 150 and 300 nm and initial mean grain sizes of 62 ± 26 nm and 104 ± 40 nm, respectively, were strained in tension at strain rates ranging from approximately 10^{-5} to $10^{-3}\,s^{-1}$. All mechanical responses presented in this letter represent those of specimens undergoing stress-assisted grain growth as a result of the applied deformation, as was reported in Ref. [6]. Representative material responses for these experiments are demonstrated in Figure 1. Post-mortem transmission electron microscopy (TEM) was employed to measure grain size distributions before and after deformation; all distributions presented here represent a minimum of 300 grain measurements.

Grain size distributions for both as-deposited and deformed 300 nm films are shown in Figure 2 in the form of a cumulative distribution function $F(d)$, where F is defined as the proportion of the area fraction of grains less than or equal to a given grain size d. It is apparent from these microstructural observations that there is a clear evolution of grain size, namely discontinuous grain growth, upon monotonically deforming to tensile failure at the two strain rates represented in Figure 2. Measurements of the grain size in the ear of these deformed specimens, where stresses are significantly lower, show no grain growth, which highlights the significance of stress as a driving force for GB migration. Examination of the distribution functions for the two specimens deformed at strain rates of 5×10^{-5} and $2 \times 10^{-3}\,s^{-1}$ also shows a significant difference; the area fraction of grains that is less than a given grain size is consistently lower for the specimen deformed at the higher strain rate. In other words, more grain growth is observed at the higher strain rate. An upper limit on the maximum grain size, which scales as approximately two to three times the film thickness, was observed as is expected for thin film geometries [18]. As a result, the upper and lower bounds for the grain size are pinned, and once this maximum grain size is achieved a stagnation effect is introduced and the distribution evolves accordingly.

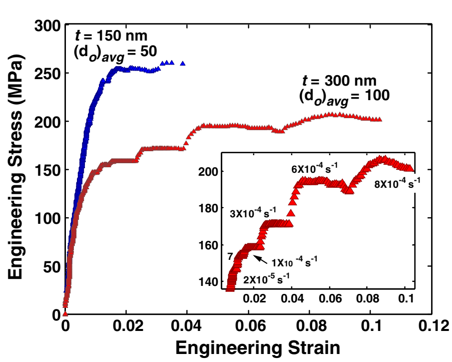

Figure 1. Representative strain rate jump tensile experiments for both 150 and 300 nm films. The inset shows a zoomed region of the first several strain rate jumps for the 300 nm film.

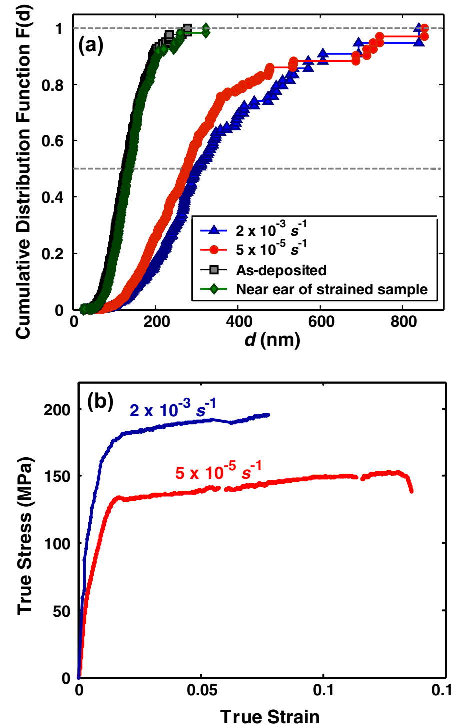

Figure 2. (a) Grain size distributions as measured from TEM micrographs, where $F(d)$ is defined as the area fraction at a given grain size that is less than that grain size. (b) Stress strain behavior for two measured strain rates showing rate dependence of 300 nm films.

The representative mechanical response for these two strain rates is also shown in Figure 2. The expected behavior for rate sensitive thermally activated deformation in metals is observed; higher applied strain rates result in higher flow stresses. Face-centered cubic (fcc)-like rate sensitive behavior that shows variations in work hardening response is measured in the early stages of deformation, but the rate dependence of work hardening is much less pronounced beyond several per cent strain. Here, the absolute value of the flow stress is rate sensitive but the rate of work hardening is not. This combination of behavior suggests that classical dislocation storage mechanisms (e.g. forest cutting) are not operative. Moreover, specimens deformed at lower strain rates demonstrate higher tensile elongations but less grain growth. These observations underscore the importance of stress, over strain, in controlling grain growth and are analogous to investigations of stress-assisted grain growth in bulk nc-Cu at cryogenic and room temperatures [9]. In the nc-Cu study, grain growth is highest at cryogenic temperatures, where the material is subjected to significantly higher stresses. Taken as a whole these observations indicate that the cause of grain growth is primarily stress-driven, rather than being governed by thermally activated processes.

The dependence of the flow stress on the applied strain rate is quantitatively illustrated in Figure 3 in the form of a double-logarithmic plot. The strain rate sensitivity m can be obtained from such a plot as defined in Eq. (2), and values are shown as measured from strain rate jump tests for 150 nm films and from jump and monotonic tests for 300 nm films in Figure 3. These values are listed as activation volumes in Table 1. Fcc nc-metals have been reported to possess m values that are up to an order of magnitude larger than those measured for coarse-grained metals [19–25]; typical values for m range from 0.02 to 0.06 for nc-Cu [20,25] and 0.005–0.02 for nc-Ni [23,24]. This change is generally understood to be related to the fundamentally different deformation mechanisms that accommodate plastic deformation in nc-metals. Results from the current study show the mean value for m extracted from strain rate jump tests of 150 nm Al films to be 0.04. The 300 nm films exhibited higher strain rate sensitivities than the 150 nm films. Strain rate jump tests initially resulted in m values that compare to the 150 nm films (~0.04), but m increased to a value of 0.14 at higher strains, approximately two orders of magnitude larger than that of microcrystalline fcc metals [26]. Monotonic strain rate experiments yield an m value of 0.08 for a given value of plastic strain of 5%. Taken as a whole, the values measured in this study are equal to or greater than what has been reported for nc-fcc metals.

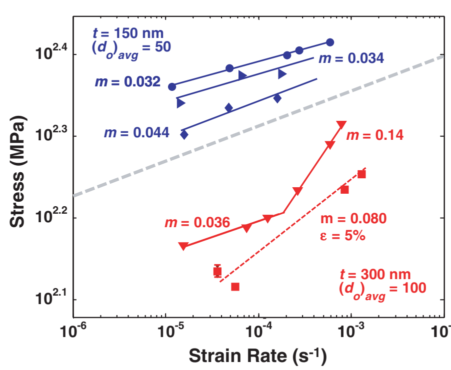

Figure 3. Strain rate sensitivity for two different film thicknesses. Data points fitted with solid line are from strain rate jump experiments while the dashed line corresponds to values measured at 5% strain during monotonic tests.

Table 1. Strain rate sensitivity parameters and activation volumes measured from experiments on nanocrystalline Al submicron thin films

Film thickness, t (nm)	Experiment	Strain rate sensitivity, m	Activation volume, v^*/b^3
150	Strain rate jump	0.037 ± 0.006	35 ± 4
300	Strain rate jump	0.036–0.14	10–55
300	Monotonic ($\varepsilon = 5\%$)	0.080	23

Activation volumes are normalized by b^3, where b is the magnitude of the Burgers vector for Al.

Because the grain size increases during deformation, one would expect the rate sensitivity to decrease towards microcrystalline-like values. Surprisingly, the opposite trend is observed. The increase in rate sensitivity with strain and grain growth points to a change in the underlying mechanisms that govern plastic flow. The current study together with observations of grain growth under the indenter in the near absence of thermal activation [9] indicate that stress-assisted grain growth is a mechanism that leads to elevated rate sensitivity in nc-Al thin films.

MD calculations were used to simulate the strain rate sensitivity of GB deformation mechanisms such as GB migration, GB sliding, and/or GB dislocation nucleation. Each of these mechanisms was investigated separately by exploring the deformation of a bicrystal at 300 K. The computational cell size for all the structures was eight atomic planes in the z-direction and approximately 12 and 9 nm in the x- and y-directions, respectively. The interatomic forces were calculated from the EAM potential of Mishin et al. [27]. The simulation boundaries in the z- and x-directions were periodic while the displacement of atoms along the top and bottom of the sample were controlled to impose the desired strain rate.

A $\Sigma11(113)$ GB with a $[1\bar{1}0]$ tilt axis, as shown in Figure 4, was selected to examine stress-assisted GB migration. Upon application of a critical shear stress, the $\Sigma11$ boundary migrated downward one (113) plane, thus inducing a plastic shear strain into the system and reducing the stress. The atomic structure of the migrated boundary was observed to remain constant after each migration step. As is shown in Figure 4, multiple simulations conducted over a range of strain rates produced reasonable stress levels and revealed a rate sensitivity for this mechanism of $m = 0.086$.

Shear induced GB migration did not occur when $\Sigma9(221)$ boundaries were sheared in the $[11\bar{2}]$ direction. Instead, they accommodated the imposed shear strain by local atomic shuffling, as previously observed in 0 K atomistic calculations [28]. These simulations were repeated over a range of strain rates and the rate sensitivity (m) of this mechanism was determined to be 0.055, as is shown in Figure 4. The shear stress needed to generate GB sliding in the $\Sigma9$ boundary was lower than the stress needed to produce GB migration in the $\Sigma11$ boundary, but both values are reasonable.

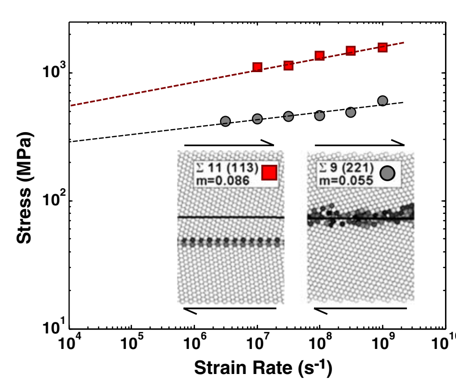

Figure 4. MD simulations showing the strain rate sensitivity of deformation due to GB sliding ($\Sigma9$) and migration ($\Sigma11$). The pictures of the two boundaries display the deformed configuration with the darker colored atoms representing those not in perfect fcc packing.

Attempts to investigate the process of dislocation nucleation from GBs were complicated by the large spatial domain required to resolve this event [29] and the long calculation times associated with low rate loading. However, it is worthwhile to note that the authors have performed calculations on the strain rate sensitivity of partial dislocation nucleation from $\Sigma 9$ and $\Sigma 11$ GBs in copper. These simulations yielded strain rate sensitivities of $m = 0.055$ and $m = 0.072$, respectively.

Although conducted at extremely high rates, these calculations suggest that the strain rate sensitivity of GB deformation mechanisms such as GB sliding, migration, and dislocation nucleation is less than it is for diffusion based mechanisms yet significantly greater than what is commonly reported for coarse grain fcc metals. Furthermore, the simulations of these boundaries and others not presented here highlight the fact that not all boundaries are prone to migration when subjected to shear stress. Thus, it seems reasonable to assume that these boundaries, along with triple junctions, play a large role in governing the stress induced microstructural evolution that is observed in nanocrystalline experiments [30]. It must be emphasized that the MD simulations were carried out at strain rates (10^6–$10^9\ s^{-1}$) many orders of magnitude higher than the experiments conducted in this work. Nevertheless, it is encouraging to note that MD predicts reasonable values for the strain rate sensitivity of GB mechanisms, which suggests that the atomic mechanisms in these simulations may be similar to those in the experiment.

The most important finding of this study is the fact that deformation in thin film nc-Al specimens undergoing stress induced grain growth is highly rate sensitive. Moreover, it is interesting to note that MD simulations suggest rate sensitivities for GB deformation mechanisms that are comparable to those measured by experiment.

This work was supported by an NSF NIRT Program (Grant No. DMR-0210215). The authors thank Prof. En Ma for fruitful and helpful discussions and Budhika Mendis for TEM assistance.

[1] B.S. Günther, A. Kumpmann, H.-D. Kunze, Scripta Metall. Mater. 27 (1992) 833.
[2] R. Mitra et al., in: Y.-W. Chung, D.C. Dunand, P.K. Liaw, G.B. Olson (Eds.), Advanced Materials for the 21st Century, Warrendale, PA, TMS, 1999, p. 553.
[3] T.R. Malow, C.C. Koch, Mater. Sci. Forum 225 (1996) 595.
[4] P.C. Millett, R.P. Selvam, A. Saxena, Acta Mater. 54 (2006) 297.
[5] J.A. Haber, W.E. Buhro, J. Am. Chem. Soc. 120 (1998) 10847.
[6] D.S. Gianola et al., Acta Mater. 54 (2006) 2263.
[7] M. Jin, A.M. Minor, E.A. Stach, J.W. Morris Jr., Acta Mater. 52 (2004) 5381.
[8] K. Zhang, J.R. Weertman, J.A. Eastman, Appl. Phys. Lett. 85 (2004) 5197.
[9] K. Zhang, J.R. Weertman, J.A. Eastman, Appl. Phys. Lett. 87 (2005) 061921.
[10] J.W. Cahn, J.E. Taylor, Acta Mater. 52 (2004) 4887.
[11] M. Yu Gutkin, I.A. Ovid'ko, Appl. Phys. Lett. 87 (2005) 251916.
[12] M. Winning, G. Gottstein, L.S. Shvindlerman, Acta Mater. 49 (2001) 211.
[13] M. Winning, G. Gottstein, L.S. Shvindlerman, Acta Mater. 50 (2002) 353.
[14] R. Schwaiger, B. Moser, M. Dao, N. Chollacoop, S. Suresh, Acta Mater. 51 (2003) 5159.
[15] L. Lu et al., Acta Mater. 53 (2005) 2169.
[16] D.S. Gianola, K.J. Hemker, M. Legros, W.N. Sharpe Jr., TMS Lett. 1 (2004) 149.
[17] G. Taylor, Prog. Mater. Sci. 36 (1992) 29.
[18] C.V. Thompson, Annu. Rev. Mater. Sci. 30 (2000) 159.
[19] R.J. Asaro, S. Suresh, Acta Mater. 53 (2005) 3369.
[20] S. Cheng et al., Acta Mater. 53 (2005) 1521.
[21] Y.M. Wang, A.V. Hamza, E. Ma, Appl. Phys. Lett. 86 (2005) 241917.
[22] Q. Wei, S. Cheng, K.T. Ramesh, E. Ma, Mater. Sci. Eng. A 381 (2004) 71.
[23] F. Dalla Torre, H. Van Swygenhoven, M. Victoria, Acta Mater. 50 (2002) 3957.
[24] Y.M. Wang, E. Ma, Appl. Phys. Lett. 85 (2004) 2750.
[25] J. Chen, L. Lu, K. Lu, Scripta Mater. 54 (2006) 1913.
[26] J. May, H.W. Höppel, M. Göken, Scripta Mater. 53 (2005) 189.
[27] Y. Mishin, D. Farkas, M.J. Mehl, D.A. Papaconstantopoulos, Phys. Rev. B 59 (1999) 3393.
[28] F. Sansoz, J.F. Molinari, Acta Mater. 53 (2005) 1931.
[29] D.E. Spearot, K.I. Jacob, D.L. McDowell, Acta Mater. 53 (2005) 3579.
[30] G. Gottstein, A.H. King, L.S. Shvindlerman, Acta Mater. 48 (2000) 397.